Towards Extra-Luminal Blood Detection from Intravascular Ultrasound Radio Frequency Data

E. Gerardo Mendizabal-Ruiz[1], George Biros[2], and Ioannis A. Kakadiaris[1]

[1] Computational Biomedicine Lab, Departments of Computer Science, Electrical and Computer Engineering, and Biomedical Engineering, University of Houston, Houston, TX
[2] Department of Biomedical Engineering and School of Computational Science and Engineering, Georgia Institute of Technology, Atlanta, GA

Abstract. Recent evidence has suggested that the presence and proliferation of vasa vasorum (VV) in the plaque is correlated to an increase in plaque inflammation and destabilization, leading to acute coronary events (e.g., heart attacks). Therefore, the detection and quantification of VV in plaque (i.e., extra luminal blood perfusion) is an important problem since it may enable the development of an index of plaque vulnerability. In this paper, we explore the feasibility of a method that employs a physics-based model of the scattered intravascular ultrasound (IVUS) radio frequency signal for the detection of blood. We evaluate our method using synthetic data and validate it using six 40 MHz pullback sequences acquired with three different IVUS systems from different arteries of rabbits and swines. Our experimental results are very promising and indicate the feasibility of our method for the computation of a feature that leads to automatic extra-luminal blood detection which may be an indication of plaque inflammation.

1 Introduction

Atherosclerosis is characterized by the formation and accumulation of plaque in the walls of the arteries which results in the hardening and thickening of the arteries [8,16]. Coronary events such as heart attacks are the result of inflammation or thrombotic complications of the plaque. Vasa vasorum (VV) is a network of microvessels that penetrate and nourish the wall of the vessel [3]. Recent evidence has suggested that the presence and proliferation (i.e., increase in density) of VV in the plaque is correlated with an increase in plaque inflammation and the processes which lead to its destabilization [7]. Based on this evidence, it is believed that the detection and measurement of VV in plaque and the detection of leakage of blood within the plaques can enable the development of an index of plaque vulnerability.

Intravascular ultrasound (IVUS) is a catheter-based medical imaging modality that is capable of providing cross-sectional images of the interior of blood vessels and is currently the gold-standard technique for assessing the morphology of blood vessels and atherosclerotic plaques *in-vivo*. The IVUS catheter consists of a miniaturized ultrasound transducer which transmits ultrasound pulses and receives its acoustic radio frequency (RF) echo signals (i.e., A-line) at a discrete set of angles. The gray-scale B-mode IVUS images are the result of postprocessing (i.e., envelope detection, compression, compensation, scaling, and geometrical transformation) of these A-line signals.

G. Fichtinger, A. Martel, and T. Peters (Eds.): MICCAI 2011, Part I, LNCS 6891, pp. 396–403, 2011.

While there have been several efforts to automatically extract and analyze the information from by IVUS data, it has not been until recent years that research has started to focus on the analysis of the RF ultrasound signals instead of the IVUS B-mode images as they are more reliable since they are not affected by any processing or transformations. Nair *et al.* [10,11] proposed a method for plaque characterization, known as "virtual histology" (IVUS-VH), that is based on the use of features extracted from the signal's power spectrum. Kawasaki *et al.* [5] proposed a tissue classification method using features computed with from integrated backscatter of the RF signal. The feasibility of using wavelet analysis for plaque characterization using the RF amplitude was studied by Katouzian *et al.* [4] and Roodaki *et al.* [15]. Recently, Ciompi *et al.* [1] presented a method for plaque characterization that enhances *in-vitro* training sets by including examples from *in-vivo* coronary plaques using a floating forward feature selection method. Korga *et al.* [6] proposed a method for plaque characterization using fractal analysis-based features of the IVUS RF signal and a k-nearest neighbor classifier. O'Malley *et al.* [12] presented a study of the feasibility of blood characterization using IVUS data by employing features based on frequency-domain measures of the high-frequency signal. A common limitation of most of these methods is that the features that characterize the tissues of interest do not consider the effects of the interactions of the sound waves with the tissues. These effects (e.g., radial attenuation and attenuation due to the medium) determine the characteristics of the RF signal along the time axis. Therefore, the validity of a set of features may not be the same for the same type of tissues at different distances from the transducer. To overcome these limitations, our group has previously presented a method for the segmentation of the lumen in IVUS data using the RF signal and a physics-based model of the received IVUS RF signal [9]. In that work, the lumen/wall interface for each transducer angle was detected by solving an inverse problem. In this paper, we explore the feasibility of a new method for the detection of blood from IVUS using a similar approach with the following differences: (i) the new method is based on the comparison of the root mean square (RMS) power of the RF IVUS signal instead of the raw B-mode data, (ii) we perform the detection of several interfaces simultaneously instead of only the lumen and wall interface, (iii) the proposed method includes a regularization term to increase stability, and (iv) the proposed method is considerably faster since the problem can be formulated as a banded linear system which can be solved very efficiently. Specifically, our contributions are: (i) an efficient method for extracting a physics-based feature for blood detection from IVUS RF data, and (ii) a method for generating pseudo-colored B-mode images based on this feature. The rest of the paper is organized as follows: Section 2 presents the methods, Section 3 presents the results obtained, Section 4 presents our discussion, and Section 5 presents our conclusions and future work.

2 Methods

2.1 Scattering Model

When an incident sound wave interacts with an object, a fraction of its power will be reflected and a fraction will be absorbed by the object. When the wavelength of the incident wave is smaller in comparison to the size of the object, the wave is reflected in all

directions (i.e., scattering). The power scattered by each object in the direction opposite to the direction of the incident wave depends on the differential backscattering cross section (DBC), which can be considered as a measurement of the effective (acoustic) area of the object [14]. The collective interaction of all the scatterers can be modeled using the Born approximation [2] which implies that the scattered echoes are weak in comparison to the incident signal, and therefore it is possible to use the principle of superposition to represent the total scattered wave as a sum of the individual reflections of each point scatterer. By considering that the wavelength of the IVUS impulse signal is large in comparison to the structures in the vessel, we can model the received IVUS RF signal by representing the structures in the vessel as a finite set of scatterers with an associated DBC coefficient. Consider a set of N point scatterers, $\Phi = \{\phi_1, \phi_2, ..., \phi_N\}$, where each scatterer $\phi_i = \{\theta_i, r_i, \tau_i\}$ is characterized by its angular position θ, its radial distance from the transducer r, and its DBC τ. An A-line signal can be modeled by computing the interaction of the impulse wave with the set of M scatterers inside an angular window $\{\Phi_\theta : (\theta - \triangle\theta) \leq \theta \leq (\theta + \triangle\theta)\}$, where $2\triangle\theta$ is the angular divergence of the ultrasound beam. The received RF signal for the transducer angular position θ can be modeled as:

$$\hat{S}_\theta(t) = \sum_{i=1}^{M} \tau_i \frac{e^{(-\mu r_i)}}{r_i} e^{\left(\frac{-(t-\frac{r_i}{c})^2}{2\sigma^2}\right)} \sin\left(\omega\left(t - \frac{r_i}{c}\right)\right), \tag{1}$$

were, $\omega = 2\pi f$ is the angular velocity of the impulse wave of frequency f, c is the speed of sound, and σ is the standard deviation of a Gaussian function that is used to approximate the envelope of the impulse function [18].

2.2 Characterization of Blood

Our hypothesis is that we can estimate the DBC value for small partitions of the IVUS RF signal and use these values to characterize and detect blood. Let $S_\theta(t)$ and $\hat{S}_\theta(t)$ be the received and modeled RF signals, respectively, for the transducer angular position θ (i.e., A-line). These signals are divided into N_P non-overlapping partitions of the same size $\triangle P = \beta_p - \alpha_p \ \forall p \in \{1, 2, ..., N_p\}$. By assuming that the signal contained on each partition $P_{\theta,p}$ is generated by a unique type of tissue, it is considered that all the scatterers that generate that signal have the same DBC $\tau_i = \tau_{\theta,p}, \forall i : \alpha_p \leq r_i < \beta_p$. To estimate the DBC value that generates the signal in each partition we propose to compute the value $\tau_{\theta,p}$ such that the quadratic error between the RMS power of the real signal $R_{\theta,p}$ and the modeled signal $\hat{R}_{\theta,p}$ for the partition $P_{\theta,p}$ is minimal. However, the characteristics of the RF signals depend on the spatial position arrangement of the scatterers, which is unknown. Similar with our previous work [9], we employ the Monte-Carlo approach on which N_s samplings of random scatterers' positions with a given density D (i.e., number of scatterers per mm^2) are used to estimate the DBC $\tau_{\theta,p}$ such that the quadratic error between the RMS power of the real and each of the sampling modeled signals $\hat{R}^s_{\theta,p}$ is minimum. Additionally, in this work we introduce a regularization term that embodies our assumptions about the variability in the DBC values of the neighboring partitions G_δ across the angular direction. Here, δ refers to

the cardinality of the neighbors and $N_n = 2\delta$ is the number of neighbors. For each partition, the DBC can be computed as:

$$\arg\min_{\tau_{\theta,p}} \sum_{s=1}^{N_s} \left(\hat{R}^s_{\theta,p}(\tau) - R_{\theta,p}\right)^2 + \beta \sum_{j \in G_\delta} \left(\tau_{\theta,p} - \tau_{j,p}\right)^2, \tag{2}$$

where β is a parameter that controls the contribution of the regularization term. The DBC for all the partitions can be efficiently computed simultaneously by solving a banded-matrix linear system.

3 Results

Synthetic data: To verify the capability of our method in recovering the DBC of the tissues of interest using the IVUS RF data, we performed experiments using synthetic IVUS RF data that were created using parameters obtained from the literature and using a mask which determine the blood and non-blood regions. The DBC values were $\tau_b = 1$ mm^2 and $\tau_w = 2$ mm^2 for blood and non-blood, respectively, while the scatterer densities were $D_b = 100$ scatterers/mm^2 and $D_w = 150$ scatterers/mm^{-2} for blood and non-blood, respectively. Since the exact values of DBC are known, it is possible to assess the sensitivity of our method with respect to the parameters such as the size of partition, number of samplings, value of the regularization term parameter, and the cardinality of the neighbors (Fig. 2). The mask used for creating the synthetic data, its corresponding IVUS B-mode reconstruction, and the recovered DBC values using 100 samplings, $\triangle P = 0.05$ *mm*, $\beta = 1$, and $\delta = 3$ are depicted in Fig. 1.

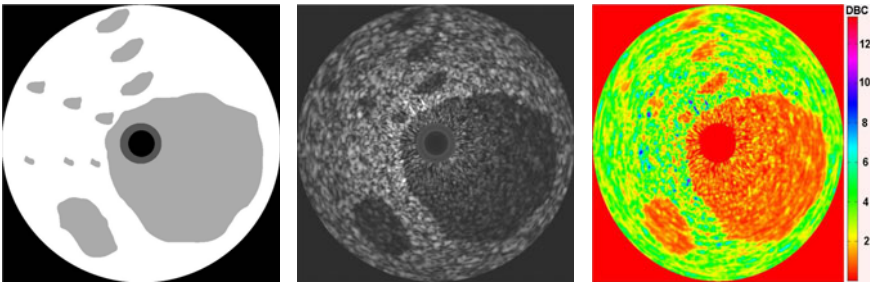

(a) (b) (c)

Fig. 1. (a) Mask used for creating the synthetic IVUS data, (b) its corresponding IVUS B-mode reconstruction, and (c) recovered DBC values using 100 samplings ($\triangle P = 0.05$ *mm*, $\beta = 1$, and $\delta = 3$)

Real RF data: Experiments were performed using real IVUS RF data from six 40 *MHz* pullback sequences acquired with three different IVUS systems. These sequences correspond to different arteries from rabbits and swines. For each sequence we employed

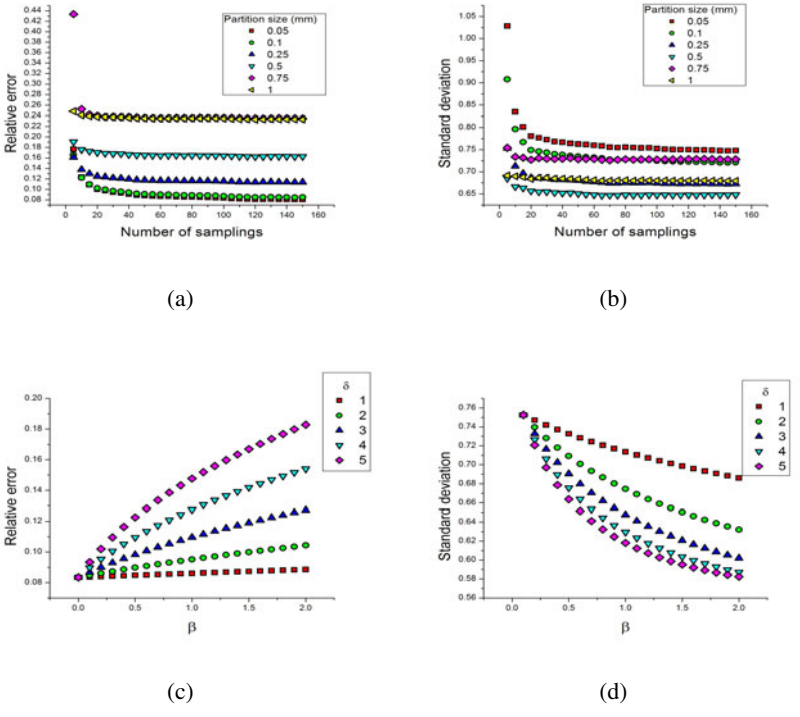

Fig. 2. (a, c) Relative error and (b, d) standard deviation for the mean of the recovered DBC values for two type of scatterers with respect to (a) the size of partition and (b) number of samplings, and (c) the cardinality of neighbors and (d) the value of the regularization term

our method on ten frames from different parts of the sequence and we compared the recovered DBC values for samples of lumen (i.e., blood) acquired from manual annotations provided by an expert. For these experiments the value of the width of the envelope of the impulse function was set to $\sigma = 5.3e^{-8}$, while the attenuation coefficient was set to the attenuation coefficient of blood (i.e., $\mu = 0.08276$ *dB/mm* [17]). The speed of sound was set to the speed of sound in a biological tissue ($c = 1540 \times 10^3$ *mm/s*). The size of partition was set to $\triangle P = 0.05$ *mm*, the density was set to $D = 400$ scatterers/mm^{-2} using the voxel approach of Rosales *et al.* [13]. The cardinality of the neighbors was set to $\delta = 3$ and $\beta = 1$. The information of the sequences and the mean of the recovered DBC values for each of the six cases are listed in Table 1.

As a preliminary blood detection experiment, we used our method to recover the DBC values from the IVUS RF data of a frame corresponding to a 40 *MHz* IVUS from swine (Fig. 3(a)), for which histological information is available. The regions corresponding to vascularization in the histology data have been annotated by an expert. The resulting DBC values for each pixel of the corresponding B-mode image are depicted using a color palette. Additionally, we created a pseudo-colored version of the IVUS image (Fig. 3(d)) using the DBC values and the same color representation. For

Table 1. Information of the sequences used for the experiments, and mean recovered DBC values for blood (τ_b) for each sequence

ID	Specimen	Artery	IVUS system	$\tau_b \times 10^{-3}$ (mm^2)	std $\times 10^{-3}$
1	Swine	Illiac	1	5.2	0.59
2	Swine	RCA	1	5.5	1.84
3	Swine	LAD	2	6.4	0.28
4	Swine	LAD	2	5.7	0.30
5	Rabbit	Aorta	3	5.5	0.56
6	Rabbit	Aorta	3	6.0	1.7

comparison, we have manually annotated the regions of the resulting image that correspond to vascularization based to the criterion that a vessel should contain a region with DBC values corresponding to blood surrounded by DBC values corresponding to non-blood. In Fig. 3(c) it can be observed that the recovered DBC values corresponding to blood from the lumen and the vessels in the adventitia are very similar. However, although there might be a correspondence between the VV in plaque (indicated by the blue rectangle in Fig. 3(b)) and some of the regions inside the plaque in the reconstructed images, we consider that the DBC might not be sufficient to detect such small vasculature by itself and should be considered along with other features.

4 Discussion

The size of the partition is a parameter that determines the size of the smallest structure that we can detect with our method. Moreover, from the synthetic data results it can be observed that, as the size of the partition decreases, the error between the recovered and true DBC values also decreases. However, the variability of the recovered DBC values increases as the size of the partition decreases. This variability is compensated with the regularization term. In the experiments with real data, the recovered DBC values for blood are similar for all the cases, which is an indication of the feasibility of using this approach for blood detection. By using a color map with the recovered DBC values, it is possible to generate pseudo colored IVUS images as the example depicted in Fig. 3(d), which may help the physicians to easier identify the different vessel structures. Exact correspondence between a histological slide and an IVUS image is difficult due to the variability in the orientation and position of the catheter and transducer. However, a fair correspondence may be achieved by locating large structures (side vessels) as in our histological example. While Figs. 3 (a, b, c) offer evidence of the feasibility of our method for extra-luminal blood detection, the manual detection of small vasculature such as VV in the recovered DBC or the colored B-mode images remains a difficult task. Therefore, a limitation of the present method is the lack of an automatic method for detecting the vasculature. We believe that the extra-luminal blood detection method can be improved by using the recovered DBC along with other image or RF-based features.

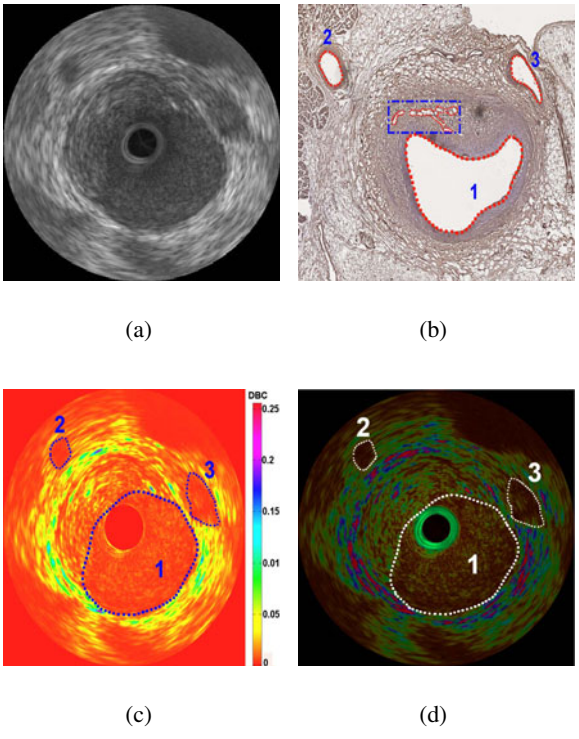

Fig. 3. (a) B-mode Cartesian frame of a 40 *MHz* IVUS swine case, (b) its corresponding histology, (c) recovered DBC values, and pseudo colored B-mode image obtained using the recovered DBC values. The main vasculature has been annotated by an expert observer on (b, c, and d).

5 Conclusions

We have presented a new method that employs a physics-based model of the IVUS RF signal for the computation of the DBC of the scatterers that generates the IVUS RF data. Our results are very encouraging and we believe that further research in this direction will lead to the development of a fast and reliable method for extra-luminal blood detection. Future work includes the use of overlapping partitions, additional quantitative validation, a method for the automatic segmentation of the vasculature, improvements to the scatterer model (i.e., adding attenuation by absorption), and the use of machine learning techniques for automatic blood detection.

References

1. Ciompi, F., Pujol, O., Leor, O., Gatta, C., Vida, A., Radeva, P.: Enhancing in-vitro IVUS data for tissue characterization. In: Proc. 4th Iberian Conference on Pattern Recognition and Image Analysis, Povoa de Varzim, Portugal, June 10-12, pp. 241–248 (2009)
2. Fontaine, I., Bertrand, M., Cloutier, G.: A system-based approach to modeling the ultrasound signal backscattered by red blood cells. Biophysical Journal 77(5), 2387–2399 (1999)

3. Heistad, D.D., Marcus, M.L.: Role of vasa vasorum in nourishment of the aorta. Blood Vessels 16, 225–238 (1979)
4. Katouzian, A., Baseri, B., Konofagou, E.E., Laine, A.F.: An alternative approach to spectrum-based atherosclerotic plaque characterization techniques using intravascular ultrasound (IVUS) backscattered signals. In: Proc. 2nd MICCAI Workshop on Computer Vision for Intravascular and Intracardiac Imaging, New York, NY (2008)
5. Kawasaki, M., Takatsu, H., Noda, T., Sano, K., Ito, Y., Hayakawa, K., Tsuchiya, K., Arai, M., Nishigaki, K., Takemura, G., Minatoguchi, S., Fujiwara, T., Fujiwara, H.: In vivo quantitative tissue characterization of human coronary arterial plaques by use of integrated backscatter intravascular ultrasound and comparison with angioscopic findings. Circulation 105, 2487–2492 (2002)
6. Koga, T., Uchino, E., Tanaka, Y., Suetake, N., Hiro, T., Matsuzaki, M.: Tissue characterization of coronary plaque by using fractal analysis-based features of IVUS RF-signal. In: Proc. 5th International Workshop on Computational Intelligence and Applications, Hiroshima, Japan, November 10-12, pp. 77–81 (2009)
7. Langheinrich, A.C., Michniewicz, A., Sedding, D.G., Walker, G., Beighley, P.E., Rau, W.S., Bohle, R.M., Ritman, E.L.: Correlation of vasa vasorum neovascularization and plaque progression in aortas of apolipoprotein E(-/-)/low-density lipoprotein(-/-) double knockout mice. Arteriosclerosis, Thrombosis, and Vascular Biology 26(2), 347–352 (2006)
8. Maton, A.: Human biology and health. Prentice Hall, Englewood Cliffs (1993)
9. Mendizabal-Ruiz, E., Biros, G., Kakadiaris, I.A.: An inverse scattering algorithm for the segmentation of the luminal border on intravascular ultrasound data. In: Proc. 12th International Conference on Medical Image Computing and Computer Assisted Intervention, London, UK, September 20- 24, pp. 885–892 (2009)
10. Nair, A., Kuban, B., Tuzcu, E., Schoenhagen, P., Nissen, S., Vince, D.: Coronary plaque classification with intravascular ultrasound radiofrequency data analysis. Circulation 106(17), 2200–2206 (2002)
11. Nair, A., Margolis, M., Kuban, B., Vince, D.: Automated coronary plaque characterisation with intravascular ultrasound backscatter: Ex vivo validation. Eurointervention 3(1), 113–120 (2007)
12. O'Malley, S.M., Naghavi, M., Kakadiaris, I.A.: One-class acoustic characterization applied to blood detection in IVUS. In: Proc. 10th International Conference on Medical Image Computing and Computer Assisted Intervention, Brisbane, Australia, October 29 - November 2, pp. 202–209 (2007)
13. Ramirez, M., Radeva, P., Mauri, J., Pujol, O.: Simulation model of intravascular ultrasound images. In: Proc. 7th International Conference on Medical Image Computing and Computer-Assisted Intervention, Saint-Malo, France, September 26 - 30, pp. 200–207 (2004)
14. Reeder, B.: Acoustic scattering by axisymmetric finite-length bodies with application to fish: measurement and modeling. Ph.D. thesis, Massachusetts Institute of Technology (2002)
15. Roodaki, A., Taki, A., Setarehdan, S.K., Navab, N.: Modified wavelet transform features for characterizing different plaque types in IVUS images; a feasibility study. In: Proc. 9th International Conference on Signal Processing, Beijing, China, October 26 - 29, pp. 789–792 (2008)
16. Ross, R.: The pathogenesis of atherosclerosis: A perspective for the 1990s. Nature 362, 801–809 (1993)
17. Shung, K.K., Smith, M.B., Tsui, B.: Principles of medical imaging. Academic Press, London (1992)
18. Thijssen, J., Oosterveld, B.: Perfomance of echographic equipment and potentials for tissue characterization. Mathematics and Computer Science in Medical Imaging F39, 455–468 (1998)